Exploring the viability of a pseudo-Nambu-Goldstone boson as ultralight dark matter in a mass range relevant for strong gravity applications

António P. Morais,[1,2,*] Vinícius Oliveira,[2,3,†] António Onofre,[4,‡] Roman Pasechnik,[5,§] and Rui Santos[6,7,‖]

[1]*Theoretical Physics Department, CERN, 1211 Geneva 23, Switzerland*
[2]*Departamento de Física, Universidade de Aveiro and Centre for Research and Development in Mathematics and Applications (CIDMA), Campus de Santiago, 3810-183 Aveiro, Portugal*
[3]*Departamento de Física, Universidade Federal da Paraíba, Caixa Postal 5008, 58051-970, João Pessoa, Paraíba, Brazil*
[4]*Centro de Física das Universidades do Minho e do Porto (CF-UM-UP), Universidade do Minho, 4710-057 Braga, Portugal*
[5]*Department of Physics, Lund University, SE-22100 Lund, Sweden*
[6]*ISEL—Instituto Superior de Engenharia de Lisboa, Instituto Politécnico de Lisboa, 1959-007 Lisboa, Portugal*
[7]*Centro de Física Teórica e Computacional, Faculdade de Ciências, Universidade de Lisboa, Campo Grande, Edifício C8 1749-016 Lisboa, Portugal*

(Received 21 February 2024; accepted 1 July 2024; published 6 August 2024)

We study a simple extension of the Standard Model featuring a dark sector with an ultralight pseudo-Nambu-Goldstone boson as a dark matter candidate. We focus on the mass range $\mathcal{O}(10^{-20}$–$10^{-10})$ eV, relevant for strong gravity applications, and explore its production and evolution in the early Universe. The model is formulated in such a way that dark matter does not couple directly to photons or other Standard Model particles avoiding some of the most stringent cosmological bounds related to axionlike particles. In this work, two different scenarios are considered depending on whether dark matter is produced in a preinflationary or postinflationary regime. We also discuss the effect from emergent topological defects such as cosmic strings and domain walls and estimate the spectrum of stochastic gravitational waves produced by their decay, enabling us to test the model at current and future gravitational-wave experiments.

DOI: 10.1103/PhysRevD.110.035008

I. INTRODUCTION

There are remarkable amounts of evidence about the existence of a Dark Matter (DM) component in the Universe [1], amounting to 27% of its total energy density [2,3]. A viable candidate must be electrically neutral (at least effectively [4]), cosmologically stable, and nonrelativistic during the period of matter-radiation equality. Among such candidates, weakly interacting massive particles (WIMPs) have been broadly studied and became widely popular due to their weak scale nature [5–7]. However, with the lack of both direct and indirect experimental evidence for WIMPs, the scientific community has been gradually increasing its attention to alternative candidates [7,8], such as axionlike particles (ALPs) [9]. The latter can emerge in various contexts [10–15] and provide an excellent solution for both thermal and nonthermal DM [16–18].

Ultralight scalar particles such as ALPs are also well motivated in the context of strong gravity (SG). In general, relativistic ultralight bosons (scalars or vectors) can form self-gravitating lumps achieving a compactness comparable to that of black holes [19–23] typically described in the context of general relativity minimally coupled to the bosonic field. A number of studies by the SG community developed in recent years, see, e.g., Refs. [24–44], postulate that such particles account for, at least, a fraction of the observed DM abundance in the Universe. In this article, focusing on the case of a real pseudo-Nambu-Goldstone Boson (pNGB), we explore under which circumstances such an assumption is valid. In particular, we discuss DM production mechanisms valid in the mass range of interest for SG scenarios, its relic abundance in the same region, and the impact of cosmological and SG constraints. Last but not least, we investigate whether an ultralight pNBG

*Contact author: aapmorais@ua.pt
†Contact author: vlbo@academico.ufpb.br
‡Contact author: antonio.Onofre@cern.ch
§Contact author: roman.pasechnik@hep.lu.se
‖Contact author: rasantos@fc.ul.pt

Published by the American Physical Society under the terms of the Creative Commons Attribution 4.0 International license. Further distribution of this work must maintain attribution to the author(s) and the published article's title, journal citation, and DOI. Funded by SCOAP³.

can be associated to additional observables such as a stochastic gravitational waves background (SGWB) from the decay of long-lived topological defects [45–49] and in which frequency range it can be tested.

A comprehensive study of simple Standard Model (SM) extensions relevant for SG applications was carried out in Ref. [50]. In this article, we focus on what was denoted as Model 1 in Table 1 of Ref. [50], in which, in addition to the SM particle content, it also contains a new *CP*-even Higgs boson, h_2, and an ultralight real pNGB denoted as θ. In the SG context, the latter were studied, e.g., in Refs. [40–44] and can lead to the formation of astrophysical objects such as oscillatons [51–53]. These are slightly time dependent and decay but can be very long lived, at least for the case of spherical stars [54]. With recent LIGO and Virgo data, searches for evidence of superradiance instabilities in the form of a SGWB [55–58] have excluded the mass of real pNGB in the range $[1.3, 17] \times 10^{-13}$ eV. While this type of DM candidate has already been studied in other contexts [59–61], in this article, we make the first study directly targeted at the mass range relevant for SG, i.e., $\sim\mathcal{O}(10^{-20}$–$10^{-10})$ eV. The presence of a $\mathcal{Z}_2$ discrete symmetry forbids direct couplings to photons of the form $\theta F^{\mu\nu}F_{\mu\nu}$, thus avoiding leading-order cosmological bounds [62] related to ALPs.

This article is organized as follows. In Sec. II, we revisit the key aspects of the model. In Sec. III, we discuss the production mechanisms viable in both pre- and postinflationary regimes. In Sec. IV, we study the implications for the SGWB produced through the decay of topological defects; lastly, we draw our conclusions in Sec. V.

II. MODEL

In this section, we revisit the basic details of Model 1 in Ref. [50], in which it was presented in greater detail. This consists of an extension of the SM with an additional complex singlet ϕ charged under a global $\mathrm{U}(1)_\mathrm{G}$ symmetry such that the scalar potential

$$V(H,\phi) = V_0(H) + \mu_\phi^2\phi\phi^* + \frac{1}{2}\lambda_\phi|\phi\phi^*|^2 + \lambda_{H\phi}H^\dagger H\phi\phi^* + V_{\mathrm{soft}}, \tag{1}$$

invariant under the transformation

$$\phi \to e^{i\alpha}\phi. \tag{2}$$

In Eq. (1), $V_0(H)$ denotes the SM potential

$$V_0(H) = \mu_H^2 H^\dagger H + \frac{1}{2}\lambda_H(H^\dagger H)^2, \tag{3}$$

and V_{soft} is a term that softly breaks the $\mathrm{U}(1)_\mathrm{G}$ global symmetry

$$V_{\mathrm{soft}} = \frac{1}{2}\mu_s^2(\phi^2 + \phi^{*2}). \tag{4}$$

The NGB field is described as a phase, θ, of the field ϕ,

$$\phi = \frac{1}{\sqrt{2}}(\sigma + \nu_\sigma)e^{i\theta/\nu_\sigma}, \tag{5}$$

where σ represents radial quantum fluctuations about the vacuum expectation value (VEV) ν_σ. The soft breaking term, Eq. (4), is responsible for generating a mass to the NGB, proportional to μ_s. As will be clear later, we are interested in the scenario where $\nu_\sigma \gg \nu_h$, where $\nu_h = 246$ GeV is the usual SM Higgs doublet VEV in the SM. The mass matrix for the physical states (h, σ, θ) reads as

$$\boldsymbol{M}^2 = \begin{pmatrix} v_h^2\lambda_H & v_h v_\sigma \lambda_{H\phi} & 0 \\ v_h v_\sigma \lambda_{H\phi} & v_\sigma^2\lambda_\phi & 0 \\ 0 & 0 & -2\mu_s^2 \end{pmatrix}, \tag{6}$$

where $\boldsymbol{M}^2$ can be diagonalized by the orthogonal transformation

$$\boldsymbol{m}^2 = \boldsymbol{O}^\dagger\boldsymbol{M}^2\boldsymbol{O} = \begin{pmatrix} m_{h_1}^2 & 0 & 0 \\ 0 & m_{h_2}^2 & 0 \\ 0 & 0 & m_\theta^2 \end{pmatrix}, \tag{7}$$

with

$$\boldsymbol{O} = \begin{pmatrix} \cos\alpha & \sin\alpha & 0 \\ -\sin\alpha & \cos\alpha & 0 \\ 0 & 0 & 1 \end{pmatrix}. \tag{8}$$

The eigenvalues of the mass matrix are

$$m_{h_{1,2}}^2 = \frac{1}{2}\left[v_h^2\lambda_H + v_\sigma^2\lambda_\phi \mp \sqrt{v_h^4\lambda_H^2 + v_\sigma^4\lambda_\phi^2 + 2v_h^2v_\sigma^2(2\lambda_{H\phi}^2 - \lambda_H\lambda_\phi)}\right], \tag{9}$$

$$m_\theta^2 = -2\mu_s^2, \tag{10}$$

and the scalar mixing angle α satisfies

$$\tan(2\alpha) = \left(\frac{2\lambda_{H\phi}\nu_h\nu_\sigma}{\lambda_H\nu_h^2 - \lambda_\phi\nu_\sigma^2}\right). \tag{11}$$

In what follows, we fix h_1 to be the SM Higgs boson with a mass of 125 GeV. The couplings between h_1, h_2, and θ with the remaining SM particles are shown in Ref. [50]. The mass of the second scalar (h_2) is a free parameter of the model. However, as discussed below, the hierarchy $\nu_\sigma \gg \nu_h$ is necessary in order to produce θ as DM, which results in

$m_{h_2} \gg m_{h_1}$. This further results in an extremely suppressed coupling of h_2 and θ to the SM particles, preventing them from reaching thermal equilibrium in the early Universe. The physical quartic couplings read as

$$\lambda_{\theta\theta\theta\theta} = -\frac{m_\theta^2}{6\nu_\sigma^2}, \tag{12}$$

where $\lambda_{\theta\theta\theta\theta} < 0$ indicates an attractive ultralight DM scenario, instead of a repulsive one, as discussed in Ref. [63].

The current LHC constraints coming from precise Higgs couplings measurements impose an upper bound on the scalar mixing angle α of Eq. (8), which can be translated into $|\sin\alpha| \lesssim \mathcal{O}(0.1)$ [64,65]. Furthermore, due to the mass hierarchy $m_{h_2} \gg m_{h_1}$, the only contribution to the invisible decay width of the 125 GeV Higgs boson is the channel $h_1 \to \theta\theta$. In the limit where $m_\theta \sim 0$ eV, the partial decay width of a Higgs boson for such a channel can be cast as [50]

$$\Gamma_{h_1\to\theta\theta} = \frac{1}{32\pi^2}\frac{m_{h_1}^3}{\nu_\sigma^2}\sin^2\alpha. \tag{13}$$

Thus, the constraint on the scalar mixing angle discussed above imposes a lower bound on the VEV, of $\nu_\sigma > 75$ GeV, which is well bellow the ranges of ν_σ relevant for this work (see the discussion in Sec. III), and the mixing between h_1 and h_2 can safely be ignored.

III. DARK MATTER

As discussed above, the mass range of interest in this article is $m_\theta \sim \mathcal{O}(10^{-20}$–$10^{-10})$ eV. The latest bounds on light axions [66] point to masses that cannot be below 2×10^{-20} eV. On the other hand, the bound could be weaker if our candidate does not represent the total amount of DM [67]. Additionally, when $m_\theta \sim 10^{-33}$ eV, which is approximately the value of the Hubble constant today, θ behaves like dark energy [68].

An ultralight scalar DM can be produced in the early Universe mainly through four different mechanisms [14]: the misalignment mechanism [4,69–73], the decay of thermal relics [74], thermally (via freeze-out) [14,75,76], and via the decay of topological defects [77]. The misalignment mechanism and the decay of topological defects are widely studied in the context of the QCD axion [14,70–72,78], whose results are also applicable for a pNGB. If thermally produced, ultralight DM [79,80] can become hot and jeopardize the period of structure formation [81]. It follows from $\nu_\sigma \gg \nu_h$ that the DM candidate considered in this article is neither produced by the decay of thermal relics nor via freeze-out as the couplings between the DM and SM particles are strongly suppressed. Other mechanisms, for instance freeze-in [82], also provide negligible contributions due to tiny portal couplings between the Higgs boson and the dark sector.

To understand how θ is produced, let us briefly revisit the pNGB cosmology at the early Universe. Our DM candidate, θ, emerges as a NGB when the global $U(1)_G$ symmetry is spontaneously broken, occurring at early times when $T \sim \nu_\sigma$ [14,76,83], and acquires a tiny mass via the soft term V_{soft}, becoming a pNGB. The spontaneous symmetry breaking (SSB) may happen before the end of inflation (we call it scenario I) or after it (scenario II), with very different consequences. We will now address in detail the two scenarios.

The temperature of the Universe at the time of inflation is given by the Gibbons-Hawking expression [14,76,84]

$$T_I = \frac{H_I}{2\pi}, \tag{14}$$

where H_I is the inflationary Hubble parameter with an upper bound that comes from the Planck and BICEP2 [14,85] measurements,

$$H_I < 8.8\times10^{13}\ \text{GeV}. \tag{15}$$

However, it is important to note that H_I can be smaller and that its value depends on which inflationary landscape is being considered [86,87].

When the global $U(1)_G$ symmetry is spontaneously broken, θ can acquire any random initial value in the range $(0, 2\pi]$. If SSB occurs before the end of inflation (scenario I), the initial values belong to different and causally disconnected patches of the Universe. Rapid expansion during inflation dilutes away the phase transition relics, and contributions from topological defects are washed out [4,14,69,88]. In scenario I, the observable Universe originates from a single causally connected region at the time of SSB featuring a single initial field value for the pNGB, whose relic abundance is dominated by the misalignment mechanism.

On the other hand, if SSB happens after the end of inflation (scenario II), the pNGB field will acquire different randomly chosen values in different causally disconnected regions of the Universe. In this case, the formation of cosmic strings is expected [76,89], that can later decay and produce DM. Additionally, if the potential has N distinct degenerate minima in θ, the formation of domain walls (DWs) [14,76] will occur. When $N > 1$, stable DW are produced, as is our case with $N = 2$. The energy density of stable DWs evolves slower than radiation and matter, and it can dominate the energy density of the Universe. This is the so-called DW problem [90], which will be further discussed below. There is a large controversy about the appropriate approach to determine the production of ultralight particles (and, in particular, ALPs) from topological defects [91]. In our analysis, we simply provide an estimate of such a contribution. For the case of scenario II, the relic abundance of θ is produced via the misalignment mechanism and through the decay of topological defects.

The soft-breaking term in the broken phase of ϕ can be cast as

$$V_{\rm soft} = \frac{\mu_s^2}{2}(\sigma+\nu_\sigma)^2 \cos\left(2\frac{\theta}{\nu_\sigma}\right). \tag{16}$$

It is clear that the potential has $N=2$ degenerate minima given by $\theta \to \theta + 2\pi\nu_\sigma k/N$, where $k=0,1$, which makes the theory invariant under a remnant discrete $\mathcal{Z}_2$ symmetry. The latter emerges upon SSB of $\mathrm{U}(1)_{\rm G}$, with the pNGB transforming as $\theta \to -\theta$. We now define the so-called misalignment angle [14] as

$$\Theta(x) \equiv \frac{\theta(x)}{\nu_\sigma/2}. \tag{17}$$

We can expand the soft-breaking term [Eq. (16)] near to the minimum and for simplicity consider only the first term in the angle

$$V_{\rm soft} \simeq \frac{1}{8} m_\theta^2 \nu_\sigma^2 \Theta^2. \tag{18}$$

This means that as a first approximation we disregard the anharmonic terms, which become important only for large value of Θ [77,92–94], which is not our case as $|\Theta| \ll 1$ in order to represent the total DM density.

The equation of motion for Θ can be obtained by varying the action, $S = \int d^4x R^3 \mathcal{L}$, where R is the scale factor, and for the Friedmann-Robertson-Walker metric, we obtain

$$\ddot{\Theta} + 3H\dot{\Theta} + m_\theta^2 \Theta = 0, \tag{19}$$

which is an equation similar to the one describing the harmonic oscillator with time dependent friction. We note that θ is naturally stable; therefore, the decay-type term, $\Gamma_\theta \dot{\Theta}$, is absent in Eq. (19) [76]. Although σ couples to θ in general, such an interaction is small enough to assume that the fields are approximately decoupled. This condition, together with the differential equation above, places us in the exact same scenario as the θ misalignment production in the axion scenario.

After the SSB of $\mathrm{U}(1)_{\rm G}$, the pNGB field assumes some initial nonzero value, $\theta_{\rm ini}$. Then, as the initial value of θ is not necessarily aligned with the minimum of the potential, the pNGB field rolls down the potential and begins to oscillate coherently when $m_\theta \simeq 3H(T_{\rm osc})$ [14], at some temperature given by[1]

$$T_{\rm osc} \simeq 1.5\ \mathrm{keV}\left(\frac{m_\theta}{10^{-20}\ \mathrm{eV}}\right)^{1/2}\left(\frac{3.9}{g_*(T_{\rm osc})}\right)^{1/4}, \tag{20}$$

[1]In this work, we assume the Standard Cosmology scenario, where the early Universe is dominated by radiation, with $H \simeq 1.66\sqrt{g_*}T^2/M_{\rm Pl}$, after inflation ($M_{\rm Pl}$ is the Planck mass).

where $g_*(T_{\rm osc})$ denotes the effective number of degrees of freedom at $T = T_{\rm osc}$, with $T_{\rm osc}$ greater than the temperature of the matter-radiation equality ($T_{\rm eq} \sim 1$ eV) [14,69,91]. This in turn allows us to extract a lower bound on m_θ,

$$m_\theta \gtrsim 4.5 \times 10^{-27}\ \mathrm{eV}, \tag{21}$$

which is consistent with the preferred range for SG applications.

The energy density originating from the coherent oscillation of θ at the minimum of the potential contributes to the final energy density of DM. This mechanism is called misalignment [14] and occurs in both scenarios I and II. After this brief discussion about the pNGB cosmology, we will now estimate the final relic density of θ.

A. Preinflationary scenario

The first scenario to discuss considers SSB of the $\mathrm{U}(1)_{\rm G}$ symmetry before the end of inflation (and assuming that the reheating temperature does not restore the symmetry after inflation). As we mentioned above, in this case, θ will be predominantly produced via the misalignment mechanism, and isocurvature perturbations will appear [14]. The cosmic microwave background (CMB) constrains the amplitude of the isocurvature perturbations, imposing a limit on the inflationary Hubble parameter H_I as a function of the VEV,

$$\frac{H_I}{\nu_\sigma} \lesssim 3 \times 10^{-5}|\Theta_i|. \tag{22}$$

However, as the Hubble scale at inflation is unknown, a certain degree of freedom is still allowed [69].

To determine the relic abundance of the θ field, we need to understand how its energy density has evolved during the early stages of the Universe evolution. The energy density of θ coherent oscillations can be obtained from the energy-momentum tensor [14], resulting in

$$\rho_\theta^{\rm mis} = \left(\frac{\nu_\sigma}{2}\right)^2\left[\frac{\dot{\Theta}^2}{2} + \frac{1}{2}m_\theta^2\Theta^2\right]. \tag{23}$$

Notice that Eq. (19) contains two real roots, implying that the system behaves as an overdamped oscillator. When the global $\mathrm{U}(1)_{\rm G}$ symmetry is spontaneously broken, Θ acquires an initial random value, Θ_i. At timescales before $T_{\rm osc}$, that is, when $T \gg T_{\rm osc}$, we have $\dot{\Theta} \simeq 0$, and therefore Θ is approximately constant. At a later time, when $T \ll T_{\rm osc}$, the field rolls down the potential and begins to oscillate. Since Θ is approximately constant until $T_{\rm osc}$, we can conclude that $\rho_\theta^{\rm mis}$, in Eq. (23), is also approximately constant during this period [14,76]. Therefore, we can take the energy density at $T_{\rm osc}$ to be

$$\rho_\theta^{\rm mis}(R_{\rm osc}) \simeq \frac{m_\theta^2 \Theta_i^2}{2}\left(\frac{\nu_\sigma}{2}\right)^2, \tag{24}$$

where Θ_i describes the initial misalignment angle when the field starts to oscillate. After $T_{\rm osc}$, the angle decreases behaving as nonrelativistic matter, $\rho_\theta^{\rm mis} \propto R^{-3}$. The energy density of θ at some instant after $T_{\rm osc}$ can be calculated using the redshift of the energy density in that period [14,73],

$$\rho_\theta^{\rm mis}(R) = \rho_\theta^{\rm mis}(R_{\rm osc})\left(\frac{R_{\rm osc}}{R}\right)^3 \simeq \frac{m_\theta^2 \Theta_i^2}{2}\left(\frac{\nu_\sigma}{2}\right)^2\left(\frac{R_{\rm osc}}{R}\right)^3. \tag{25}$$

As alluded to above, notice that for a given mass, m_θ, the energy density of θ is controlled by its initial value, vanishing in the case of $\Theta_i = 0$. Using the definition of entropy density and assuming that it is constant, one obtains

$$\left(\frac{R_{\rm osc}}{R_0}\right)^3 = \frac{g_s(T_0)}{g_s(T_{\rm osc})}\left(\frac{T_0}{T_{\rm osc}}\right)^3, \tag{26}$$

where $g_s(T_0) = 3.91$ and $T_0 = 2.3 \times 10^{-4}$ eV is the temperature today [95].

The DM relic density is defined as

$$\Omega_\theta h^2 = \frac{\rho_\theta^{\rm mis}(R_0)}{\rho_{\rm crit}/h^2}. \tag{27}$$

Taking $\rho_{\rm crit} = 1.05 \times 10^{-5} h^2\,{\rm GeV/cm^3} \simeq 8.15 \times 10^{-47} h^2\,{\rm GeV^4}$ [95], one can write

$$\Omega_\theta h^2 = 0.11\left(\frac{m_\theta}{10^{-20}\ {\rm eV}}\right)^{1/2}\left(\frac{\nu_\sigma}{10^{17}\ {\rm GeV}}\right)^2 \times \left(\frac{\Theta_i}{1.5 \times 10^{-1}}\right)^2 \mathcal{F}(T_{\rm osc}), \tag{28}$$

where $\mathcal{F}(T_{\rm osc}) \equiv \left(\frac{3.91}{g_s(T_{\rm osc})}\right)\left(\frac{g_s(T_{\rm osc})}{3.4}\right)^{3/4}$ varies in the range from 1 to ~0.3. This results in an upper limit on Θ_i compatible with $\Omega_\theta h^2 \leq 0.11$ that reads as

$$\Theta_i \leq 0.15\left(\frac{10^{-20}\ {\rm eV}}{m_\theta}\right)^{1/4}\left(\frac{10^{17}\ {\rm GeV}}{\nu_\sigma}\right)\mathcal{F}(T_{\rm osc})^{-1/2}. \tag{29}$$

In Fig. 1, we show the solution of Eq. (28) for three representative values of the DM mass, for instance, $m_\theta = 10^{-10}$ (blue curve), 10^{-15} (green curve), and 10^{-20} eV (red curve). As can be observed, for the mass range of interest in our discussion, it is always possible to saturate the DM relic abundance with the θ field by fixing the initial value of the misalignment angle $\Theta_i = 4.7 \times 10^{-4}, 8.4 \times 10^{-3}$, and 1.5×10^{-1} for $m_\theta = 10^{-10}$, 10^{-15}, and 10^{-20} eV, respectively.

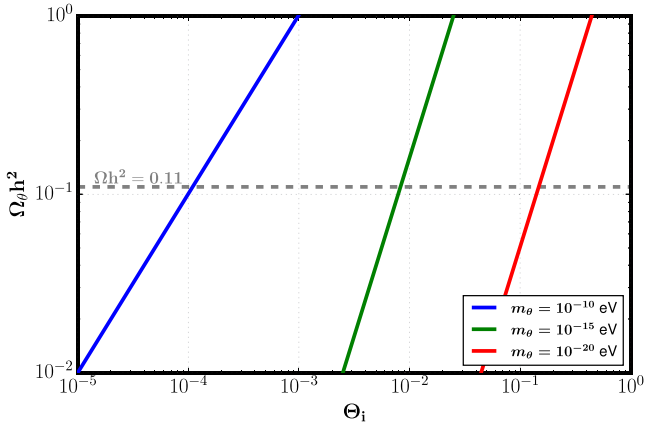

FIG. 1. Abundance of ultralight DM for the case where the SSB occurs before the end of inflation, for $m_\theta = 10^{-10}$, 10^{-15}, and 10^{-20} eV for blue, green, and red curves, respectively. Here, we fixed $\nu_\sigma = 10^{17}$ GeV.

B. Postinflationary scenario

Let us now consider the scenario where the global symmetry breaking occurs after the end of inflation, i.e., $T_I > \nu_\sigma$. As previously discussed, in this case, DM is produced through the decay of topological defects (cosmic strings and DWs) [96] besides the misalignment mechanism that is also present. Cosmic strings emerge when the $\mathrm{U}(1)_{\rm G}$ gauge symmetry is spontaneously broken at $T \sim \nu_\sigma$. After that, a potential with degenerate minima and a $\mathcal{Z}_2$ discrete symmetry arises. This symmetry, when spontaneously broken at $T_{\rm osc}$, produces DWs.

The approach to obtain the contribution from misalignment is in many aspects identical to what is described above for scenario I. However, a few differences regarding the value of Θ_i need to be accounted for. In particular, when the $\mathrm{U}(1)_{\rm G}$ symmetry is spontaneously broken, the Universe is divided into several causally disconnected patches, each of which has an independent value of Θ_i. Therefore, Θ_i is no longer a free parameter as before, and it is reasonable to consider the average of an uniform distribution [14,76,97], $\Theta_i^2 \to \langle \Theta_i^2 \rangle$, where, neglecting the anharmonic effect, one has

$$\langle \Theta_i^2 \rangle = \frac{1}{2\pi}\int_{-\pi}^{\pi} d\Theta_i \Theta_i^2 = \frac{\pi^2}{3}. \tag{30}$$

Notice that from $T_I > \nu_\sigma$ and using Eqs. (14) and (15), one can obtain the upper limit on the $\mathrm{U}(1)_{\rm G}$ breaking scale as $\nu_\sigma \lesssim 1.4 \times 10^{13}$ GeV. Thus, the contribution from the misalignment mechanism for this scenario is obtained from Eqs. (28) and (30) and can be written as

$$\Omega_\theta^{\rm mis} h^2 \simeq 1.6 \times 10^{-15}\left(\frac{m_\theta}{10^{-20}\ {\rm eV}}\right)^{1/2}\left(\frac{\nu_\sigma}{10^{9}\ {\rm GeV}}\right)^2 \mathcal{F}(T_{\rm osc}). \tag{31}$$

With the considered values for the ultralight scalar mass in a range relevant for compact astrophysical objects, the misalignment contribution to the total relic density of θ is extremely suppressed as previously noticed in other works [76,97]. Therefore, one must closely inspect the contribution from other sources such as the decay products of topological defects.

The global $U(1)_G$ symmetry breaks spontaneously when $T \sim \nu_\sigma$, which induces the formation of cosmic strings [77,98]. Such strings decay into pNGBs [76,99,100] at $m_\theta t_{\rm str} \sim 1$, and the energy stored in the cosmic strings is released dominantly into DM. The evolution of the energy density of these strings is described by the scaling solution

$$\rho^{\rm string}(t) = \xi \frac{\mu_{\rm string}}{t^2}, \tag{32}$$

where ξ represents the number of strings in a Hubble volume. We will assume $\xi \sim 1$ [101], and

$$\mu_{\rm string} = \pi \nu_\sigma^2 \log\left(\frac{t}{d}\right) \tag{33}$$

is the energy of a string per unit length, with $t = 1/H$ and $d \sim 1/m_{h_2}$ the width of the string [100].

When $H \sim m_\theta$, the $\mathcal{Z}_2$ discrete symmetry, which emerges after SSB of $U(1)_G$, breaks and leads to the formation of stable DWs [89,97]. To avoid the DW problem [90], we consider an additional generic term in the potential, δV, which slightly breaks the discrete $\mathbb{Z}_2$ symmetry and lifts the degeneracy between the two $\mathbb{Z}_2$ symmetric vacua evident in Eq. (16). Additionally, we require that $V_{\rm soft} > \delta V$ since the bias term can contribute to the θ mass. The new δV term produces a pressure on the walls and eventually annihilates them. The total potential [Eq. (1)] can then be rewritten:

$$V(H,\phi) = V_0(H) + \mu_\phi^2 \phi\phi^* + \frac{1}{2}\lambda_\phi |\phi\phi^*|^2 + \lambda_{H\phi} H^\dagger H \phi\phi^* + V_{\rm soft} + \delta V. \tag{34}$$

The δV contribution was first proposed by Sikivie in Ref. [102] and represents a pressure term [77,103–105]. Here, we are not concerned about an exact expression for δV, as our focus is rather on the difference in the values of the potential calculated at each minimum $\Delta V \simeq \delta V$ [78,106]. A detailed discussion about DWs dynamics with pressure terms can be found in Ref. [107].

When the DWs are produced, each cosmic string becomes attached to the DWs and a string-wall network emerges. As for the case of strings, numerical studies show that the energy density of the $\mathbb{Z}_2$ DWs is described by the scaling solution [105]

$$\rho^{\rm wall}(t) = A \frac{\sigma_{\rm wall}}{t}. \tag{35}$$

where $A \simeq 0.8 \pm 0.1$ is the area parameter [108] and $\sigma_{\rm wall}$ is the tension of the DW [78,109]

$$\sigma_{\rm wall} = 2 m_\theta \nu_\sigma^2. \tag{36}$$

As mentioned above, the pressure term lifts the degeneracy between the two vacua, producing a volume pressure $p_V \sim \Delta V$ on the DWs, proportional to the difference between the minima. Besides the volume pressure, DWs are also affected by a tension force $p_T \sim \sigma_{\rm wall}/t$ such that their decay occurs when $p_V \sim p_T$, which implies [97]

$$H_{\rm decay} = \frac{\Delta V}{A \sigma_{\rm wall}}. \tag{37}$$

Then, combining Eqs. (36) and (37), we obtain the temperature at which the DWs decay:

$$T_{\rm decay} \simeq 1.98 \times 10^8 \ {\rm GeV}\, A^{-1/2} \left(\frac{g_*(T_{\rm decay})}{10}\right)^{-1/4} \times \left(\frac{m_\theta}{10^{-20}\ {\rm eV}}\right)^{-1/2} \left(\frac{v_\sigma}{10^9\ {\rm GeV}}\right)^{-1/2} \left(\frac{\Delta V}{{\rm MeV}^4}\right)^{1/2}. \tag{38}$$

As DWs predominantly decay into DM and also produce gravitational waves (GWs), their presence does not conflict with the predictions of big bang nucleosynthesis (BBN). The DW's decay products, DM and GWs, do not inject energy into the Standard Model particles comprising the primordial thermal bath. Consequently, the thermal equilibrium and nucleosynthesis processes during BBN remain unaffected by the presence of DWs [14,97,105]. However, it is important to highlight that this is only true in the presence of a tiny coupling between DM and SM particles in order to avoid thermalization.[2] Therefore, to ensure compatibility with observational constraints and theoretical predictions, it is sufficient to impose a requirement that DWs decay before the epoch of matter-radiation equality, i.e., $H_{\rm decay} > H_{\rm eq}$ ($T_{\rm eq} \sim 1$ eV), which yields the condition

$$\Delta V > 2.5 \times 10^{-35}\ {\rm MeV}^4\, A \left(\frac{m_\theta}{10^{-20}\ {\rm eV}}\right) \left(\frac{\nu_\sigma}{10^9\ {\rm GeV}}\right)^2. \tag{39}$$

As we mentioned before, another lower bound on ΔV that we will impose here arises from requiring that the DWs should decay before they dominate the energy density of the Universe, which happens when $t_r \sim (G\sigma_{\rm wall})^{-1}$, where $G = 6.7 \times 10^{-39}\ {\rm GeV}^{-2}$ is the gravitational constant. Therefore, we require

[2]For a detail discussion about DWs decay and BBN, see Ref. [110].

$$\frac{1}{GA\sigma_{\rm wall}} \gg H^{-1}_{\rm decay}, \tag{40}$$

and using Eqs. (36) and (37), we obtain

$$\Delta V \gg 2.68 \times 10^{-48}\ {\rm MeV}^4\, A^2 \left(\frac{m_\theta}{10^{-20}\ {\rm eV}}\right)^2 \left(\frac{\nu_\sigma}{10^9\ {\rm GeV}}\right)^4. \tag{41}$$

Additionally, we need to ensure that DWs decay before they start dominating the energy density of the Universe as the misalignment mechanism has been required to occur during a radiation-dominated period.

As shown in Refs. [77,101,108], the DM particles produced through the decay of the DWs are mildly relativistic and become nonrelativistic before the BBN. However, a more detailed studied about the energy of pNGB produced through decay of DW needed to be developed since the results used for the pNGB scenario is obtained for axions. Some bounds on VEV of global symmetry and pNGB mass can emerge in a more detailed study, as was done in Ref. [111]. As a good approximation, we can use the results for axion to estimate the energy density of DM produced through the decay of the DWs.

As we mentioned before, the DWs predominantly decay into DM and GWs. However, as we will explore in the following section, the final amount of GWs is significantly suppressed, though it can be experimentally probed. Therefore, we will assume that at the time of DWs decay[3] $\rho^{\rm wall}_\theta(t_{\rm decay}) \simeq \rho^{\rm wall}(t_{\rm decay})$, where $\rho^{\rm wall}_\theta(t_{\rm decay})$ represents the energy density of θ produced through DWs decay. We can redshift Eq. (35), where the produced DM behaves as matter (nonrelativistic), as

$$\rho^{\rm wall}_\theta(t_0) \simeq \rho^{\rm wall}(t_{\rm decay}) \left(\frac{R(t_{\rm decay})}{R(t_0)}\right)^3, \tag{42}$$

where

$$\rho^{\rm wall}(t_{\rm decay}) = 2\sigma_{\rm wall} H_{\rm decay}. \tag{43}$$

Putting everything together, the relic density of pNGB produced via the decay of DWs is given by

$$\Omega^{\rm wall}_\theta h^2 \simeq 1.5 \times 10^{-29} A^{1/2} \left(\frac{g_*(T_{\rm decay})}{10}\right)^{-1} \left(\frac{m_\theta}{10^{-20}\ {\rm eV}}\right)^{3/2} \times \left(\frac{\nu_\sigma}{10^9\ {\rm GeV}}\right)^3 \left(\frac{\Delta V}{{\rm MeV}^4}\right)^{-1/2}. \tag{44}$$

[3]It is worth noting that, while DWs behave as nonrelativistic matter and θ produced by DWs are mildly relativistic, this relation is subject to a correction factor of order $\mathcal{O}(1)$, which represents the mean energy of pNGB radiated from DWs. For a deeper understanding on this point, see Refs. [77,101,108].

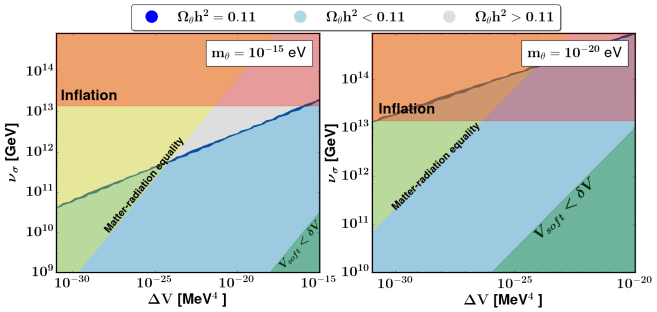

FIG. 2. Viable parameter space in the plane $(\Delta V, \nu_\sigma)$ for the scenario where the SSB occurs after the end of inflation. The correct DM relic density is achieved along the blue line, the gray region represents $\Omega_\theta h^2 > 0.11$, while the light blue means $\Omega_\theta h^2 < 0.11$. The yellow region is excluded because the necessary requirement of DWs to decay before matter-radiation equality does not hold. The green region is excluded due to $V_{\rm soft} < \delta V$. The red region represents the end of inflation.

Last but not least, the total relic density of the ultralight scalar in a regime where the global $\mathrm{U}(1)_{\rm G}$ is broken in a postinflationary era reads as

$$\Omega_\theta h^2 \simeq \Omega^{\rm mis}_\theta h^2 + \Omega^{\rm wall}_\theta h^2, \tag{45}$$

where the cosmic strings contribution is negligible, as shown in Ref. [77], and thus neglected in the remainder of this analysis.

In Fig. 2, we present the allowed parameter space in the plane $(\Delta V, \nu_\sigma)$ for the scenario where the SSB occurs after the end of inflation. The DM relic density that saturates the measured value, i.e., $\Omega_\theta h^2 = 0.11$, is achieved along the blue line. The gray region represents DM overdensity with $\Omega_\theta h^2 > 0.11$, while the light blue indicates $\Omega_\theta h^2 < 0.11$ where DM is underabundant. The yellow region is excluded, as the necessary requirement for DW decay before the matter-radiation equality does not hold. The green region is excluded due to $V_{\rm soft} < \delta V$. The red region represents the end of inflation. The left panel specializes to an ultralight scalar mass of 10^{-15} eV, while the right panel considers $m_\theta = 10^{-20}$ eV. Notice that for the latter case there are no allowed points that could explain the measured relic abundance of DM. In turn, under the conditions of a postinflationary scenario, oscillatons resulting from a clump of ultralight real scalars with mass close to 10^{-20} eV cannot be described in the context of a model where θ fully describes the DM component of the Universe, which contrasts with the preinflationary regime discussed for scenario I.

In Fig. 3, we present the allowed parameter space in the plane (m_θ, $\Omega_\theta h^2$), with the $\mathrm{U}(1)_{\rm G}$ breaking VEV, ν_σ, represented in the color bar, for the scenario where SSB occurs after the end of inflation. The white shaded region indicates the excluded mass range due to searches for superradiance instabilities in the form of a SGWB at the LIGO-Virgo experiment [57,58]. This figure corroborates

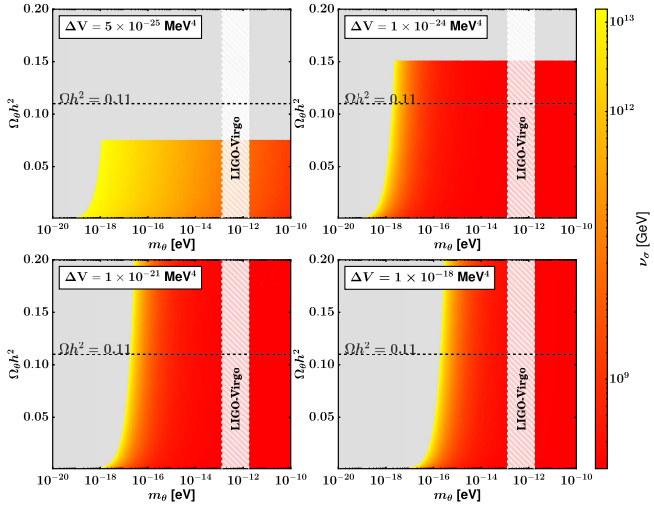

FIG. 3. Viable parameter space in the plane $(m_\theta, \Omega_\theta h^2)$, with the color bar denoting ν_σ, for the scenario where SSB occurs after the end of inflation. The white shaded region is excluded due to the constraints imposed by the LIGO-Virgo experiment in the searches for superradiance instabilities for a mass range $[1.3, 17] \times 10^{-13}$ eV [57,58].

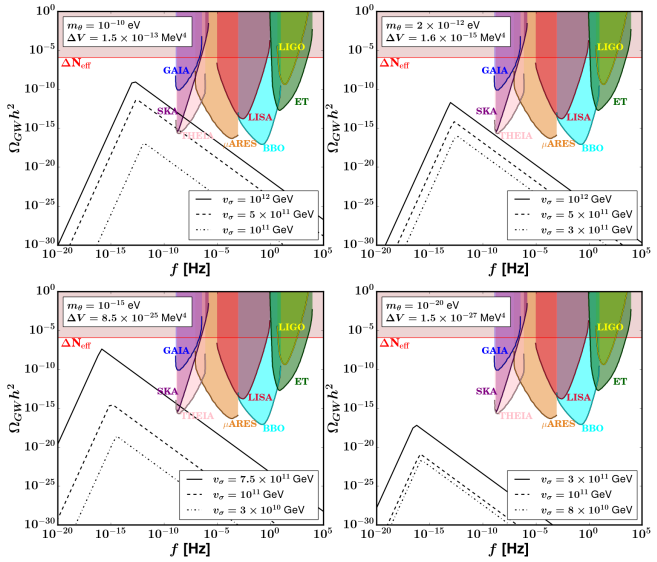

FIG. 4. GW spectrum from DWs for different values of ν_σ (black curves) where each graph represents different values of m_θ. The shaded region represents the experimental sensitivities of GAIA, SKA, μARES, LISA, BBO, LIGO, THEIA, and ET. The red shaded region is excluded due to the $\Delta N_{\rm eff}$ constraint.

the observation related to Fig. 2, where it is verified that a mass of 10^{-20} eV is not compatible with a full description of DM. Indeed, only masses larger than $\mathcal{O}(10^{-18})$ eV fulfill such a requirement as it is evident in Fig. 3. Likewise, ΔV has to be above $\mathcal{O}(10^{-24})$ MeV^4. One must also note that v_σ does not play a relevant role in the considered region.

IV. GRAVITATIONAL WAVES FROM DOMAIN WALLS

The decay of DWs can generate not only DM but also a spectrum of SGWB [78,112–114], expected with the characteristic peak frequency and amplitude features depending on the model's parameters. These can potentially be observed at current and future GW observatories, offering a unique probe of the Universe's earliest moments.

The SGWB amplitude at the peak frequency can be written as [108,109,115]

$$\Omega_{\rm GW} h^2(t_0)_{\rm peak} = 5.2 \times 10^{-20} A^4 \tilde{\epsilon}_{gw} \left(\frac{g_*(T_{\rm decay})}{10}\right)^{1/3} \times \left(\frac{\sigma}{\rm TeV^3}\right)^4 \left(\frac{\rm MeV^4}{\Delta V}\right)^2, \quad (46)$$

where $\tilde{\epsilon}_{gw} \simeq 0.7$ is the efficiency parameter and the peak frequency of the GW is given by

$$f_{\rm peak}(t_0) \simeq 3.99 \times 10^{-9}\ {\rm Hz}\ A^{-1/2} \left(\frac{\rm TeV^3}{\sigma}\right)^{1/2} \left(\frac{\Delta V}{\rm MeV^4}\right)^{1/2}. \quad (47)$$

The full spectrum is obtained by multiplying the peak amplitude by the spectral function as

$$\Omega_{\rm GW} h^2 \simeq \Omega_{\rm GW} h^2_{\rm peak} \times \begin{cases} \left(\frac{f_{\rm peak}}{f}\right), & \text{if } f > f_{\rm peak} \\ \left(\frac{f}{f_{\rm peak}}\right)^3, & \text{if } f < f_{\rm peak}. \end{cases} \quad (48)$$

In Fig. 4, we show examples of the SGWB given by Eq. (48) for different values of ν_σ. The experimental sensitivities of GAIA [116], SKA [117], LISA [118], μARES [119], BBO [120], LIGO [121], and the Einstein Telescope (ET) [122] are shown in the shaded regions. The energy density of a SGWB behaves like radiation [78]. Therefore, considering cosmological observations obtained from the PLANCK satellite and the limits on the effective number of neutrino species ($\Delta N_{\rm eff}$) derived from the CMB, one can extract an upper bound on the energy density amplitude of approximately $\Omega_{\rm GW} h^2 \lesssim 10^{-6}$. The excluded region is represented by the red shaded horizontal band on the four panels. It is clear from our results that, although the detection of a SGWB is not precluded, it is only possible for a restricted set of parameters and only at SKA and THEIA. Notice that the SGWB discussed here is of cosmological nature and not to be confused with that indicated in the vertical band of Fig. 3, which is of an astrophysical origin.

To conclude, in our analysis, we revisit in the left panel of Fig. 5 the viable parameter space in the plane $(\Delta V, \nu_\sigma)$ for $m_\theta = 10^{-15}$ eV, as already presented in Fig. 2, left panel. The added red triangles represent points that not only

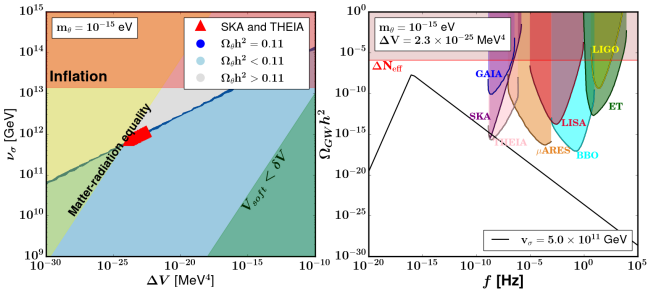

FIG. 5. Left: viable parameter space in the plane $(\Delta V, \nu_\sigma)$ for $m_\theta = 10^{-15}$ eV as already presented in Fig. 2. The red triangles represent the set of parameters that provide the correct DM abundance and within reach of the experimental sensitivity of the SKA and THEIA experiments. Right: spectrum of GWs produced from DWs, where the black curves represents a choice of parameters corresponding to one red triangle in the left panel.

saturate the DM relic abundance but can also be tested by future GW experiments such as SKA and THEIA. In the right panel, we show the spectrum of GWs produced from DWs, where the black curves represent a choice of parameters that correspond to one of the red triangles in the left panel. The red triangles correspond to what we consider the most phenomenologically interesting solution of our analysis where the model describes DM in a postinflationary regime; it can clump in the form of oscillatons and can be potentially tested in both astrophysical (LIGO-Virgo) and cosmological channels (SKA, THEIA).

V. CONCLUSIONS

We investigated a model that is a simple extension of the Standard Model by the addition of a complex singlet. When this new field acquires a nonzero VEV, a Nambu-Goldstone boson emerges. This NGB acquire mass through an additional soft breaking term in the potential becoming an pseudo-Nambu-Goldstone boson. We are focused on the scenario where the pNGB is an ultralight particle, in the mass range $\mathcal{O}(10^{-20}$–$10^{-10})$ eV, which makes it stable and therefore a good DM candidate.

Our motivation to explore this range of masses is primarily related to the strong gravity implications from the fact that ultralight relativistic bosons can clump and form objects with a compactness similar to that of black holes. With current experimental facilities, such objects are under active study and can be probed upon the measurement of an astrophysical SGWB emergent from superradiance instabilities.

We have discussed the mechanisms of DM production relevant for the considered mass range. In particular, due to extremely suppressed couplings with SM particles, DM is nonthermally produced through the misalignment mechanism and/or the decay of topological defects. However, when the breaking of the global $U(1)_G$ symmetry occurs before the end of inflation, there is no contribution from topological defects, and it takes place predominately via misalignment. Indeed, we have noted that it is always possible to find a misalignment angle that saturates the observed DM relic abundance for the entire mass range relevant for strong gravity applications. For a postinflationary regime, the main mechanism at play for DM generation is the decay of DWs. In this case, it is only possible to satisfy the entire DM relic density for ultralight scalar masses larger than approximately 10^{-16} eV. Besides the known astrophysical SGWB observables at LIGO-Virgo frequencies, the model can also offer a cosmological SGWB potentially observable at SKA and THEIA.

With this article, we expect to provide valuable information to the strong gravity community, where for the case of oscillatons their solutions can be concretely/numerically mapped to viable DM scenarios in simple extensions of the SM of particle physics.

ACKNOWLEDGMENTS

The authors gratefully thank Carlos A. R. Herdeiro, Eugen Radu and Nicolas Sanchis-Gual for insightful discussions on strong gravity connections related to the presented work. The authors also thank Fabrizio Rompineve for relevant comments related to domain walls. This work was supported by FCT Grants No. CERN/FIS-PAR/0021/2021 (https://doi.org/10.54499/CERN/FIS-PAR/0021/2021), No. CERN/FIS-PAR/0019/2021 (https://doi.org/10.54499/CERN/FIS-PAR/0019/2021), No. CERN/FIS-PAR/0024/2021 (https://doi.org/10.54499/CERN/FIS-PAR/0024/2021), No. CERN/FIS-PAR/0025/2021 (https://doi.org/10.54499/CERN/FIS-PAR/0025/2021), and No. PTDC/FIS-AST/3041/2020 (https://doi.org/10.54499/PTDC/FIS-AST/3041/2020). A. P. M. is supported by the Center for Research and Development in Mathematics and Applications (CIDMA) through the Portuguese Foundation for Science and Technology (FCT—Fundação para a Ciência e a Tecnologia), references UIDB/04106/2020 (https://doi.org/10.54499/UIDB/04106/2020) and UIDP/04106/2020 (https://doi.org/10.54499/UIDP/04106/2020), and by national funds (OE), through FCT, I. P., in the scope of the framework contract foreseen in the numbers 4, 5, and 6 of the article 23, of the Decree-Law 57/2016, of August 29, changed by Law 57/2017, of July 19 [Contract No. DL57/2016/CP1482/CT0016 (https://doi.org/10.54499/DL57/2016/CP1482/CT0016)]. V. O. acknowledgment CAPES for financial support. R. S. is supported by FCT under Contracts No. UIDB/00618/2020 (https://doi.org/10.54499/UIDB/00618/2020) and No. UIDP/00618/2020 (https://doi.org/10.54499/UIDP/00618/2020). R. P. is supported in part by the Swedish Research Council grant, Contract No. 2016-05996, as well as by the European Research Council (ERC) under the European Union's Horizon 2020 research and innovation programme (Grant No. 668679).

[1] Gianfranco Bertone and Dan Hooper, History of dark matter, Rev. Mod. Phys. **90**, 045002 (2018).

[2] N. Aghanim *et al.* (Planck Collaboration), Planck 2018 results. VI. Cosmological parameters, Astron. Astrophys. **641**, A6 (2020); Astron. Astrophys. **652**, C4(E) (2021).

[3] Manuel Drees, Dark matter theory, Proc. Sci. ICHEP2018 (**2019**) 730 [arXiv:1811.06406].

[4] Zachary Bogorad and Natalia Toro, Ultralight millicharged dark matter via misalignment, J. High Energy Phys. 07 (2022) 035.

[5] Gianfranco Bertone, Dan Hooper, and Joseph Silk, Particle dark matter: Evidence, candidates and constraints, Phys. Rep. **405**, 279 (2005).

[6] Gary Steigman, Basudeb Dasgupta, and John F. Beacom, Precise relic WIMP abundance and its impact on searches for dark matter annihilation, Phys. Rev. D **86**, 023506 (2012).

[7] Giorgio Arcadi, Maíra Dutra, Pradipta Ghosh, Manfred Lindner, Yann Mambrini, Mathias Pierre, Stefano Profumo, and Farinaldo S. Queiroz, The waning of the WIMP? A review of models, searches, and constraints, Eur. Phys. J. C **78**, 203 (2018).

[8] Leszek Roszkowski, Enrico Maria Sessolo, and Sebastian Trojanowski, WIMP dark matter candidates and searches —current status and future prospects, Rep. Prog. Phys. **81**, 066201 (2018).

[9] Prateek Agrawal *et al.*, Feebly-interacting particles: FIPs 2020 workshop report, Eur. Phys. J. C **81**, 1015 (2021).

[10] Jörn Kersten and Alexei Yu. Smirnov, Right-handed neutrinos at CERN LHC and the mechanism of neutrino mass generation, Phys. Rev. D **76**, 073005 (2007).

[11] R. D. Peccei and Helen R. Quinn, *CP* conservation in the presence of instantons, Phys. Rev. Lett. **38**, 1440 (1977).

[12] R. D. Peccei and Helen R. Quinn, Constraints imposed by *CP* conservation in the presence of instantons, Phys. Rev. D **16**, 1791 (1977).

[13] Michael Dine, Willy Fischler, and Mark Srednicki, A simple solution to the strong *CP* problem with a harmless axion, Phys. Lett. **104B**, 199 (1981).

[14] David J. E. Marsh, Axion cosmology, Phys. Rep. **643**, 1 (2016).

[15] David J. E. Marsh, Axions and ALPs: A very short introduction, in *Proceedings of the 13th Patras Workshop on Axions, WIMPs and WISPs* (2018), pp. 59–74, arXiv:1712.03018.

[16] Marco Battaglieri *et al.*, US cosmic visions: New ideas in dark matter 2017: Community report, in U.S. Cosmic Visions: New Ideas in Dark Matter (2017), arXiv:1707.04591.

[17] Asimina Arvanitaki, Masha Baryakhtar, and Xinlu Huang, Discovering the QCD axion with black holes and gravitational waves, Phys. Rev. D **91**, 084011 (2015).

[18] Lam Hui, Jeremiah P. Ostriker, Scott Tremaine, and Edward Witten, Ultralight scalars as cosmological dark matter, Phys. Rev. D **95**, 043541 (2017).

[19] David J. Kaup, Klein-Gordon Geon, Phys. Rev. **172**, 1331 (1968).

[20] Remo Ruffini and Silvano Bonazzola, Systems of self-gravitating particles in general relativity and the concept of an equation of state, Phys. Rev. **187**, 1767 (1969).

[21] Franz E. Schunck and Eckehard W. Mielke, General relativistic boson stars, Classical Quantum Gravity **20**, R301 (2003).

[22] Steven L. Liebling and Carlos Palenzuela, Dynamical boson stars, Living Rev. Relativity **15**, 6 (2012).

[23] Patrick J. Fox, Neal Weiner, and Huangyu Xiao, Recurrent axion stars collapse with dark radiation emission and their cosmological constraints, Phys. Rev. D **108**, 095043 (2023).

[24] Vitor Cardoso and Paolo Pani, Testing the nature of dark compact objects: A status report, Living Rev. Relativity **22**, 4 (2019).

[25] Vitor Cardoso, Taishi Ikeda, Rodrigo Vicente, and Miguel Zilhão, Parasitic black holes: The swallowing of a fuzzy dark matter soliton, Phys. Rev. D **106**, L121302 (2022).

[26] Juan Calderón Bustillo, Nicolas Sanchis-Gual, Alejandro Torres-Forné, José A. Font, Avi Vajpeyi, Rory Smith, Carlos Herdeiro, Eugen Radu, and Samson H. W. Leong, GW190521 as a merger of Proca stars: A potential new vector boson of 8.7×10^{-13} eV, Phys. Rev. Lett. **126**, 081101 (2021).

[27] Nicolas Sanchis-Gual, Miguel Zilhão, and Vitor Cardoso, Electromagnetic emission from axionic boson star collisions, Phys. Rev. D **106**, 064034 (2022).

[28] Liina M. Chung-Jukko, Eugene A. Lim, David J. E. Marsh, Josu C. Aurrekoetxea, Eloy de Jong, and Bo-Xuan Ge, Electromagnetic instability of compact axion stars, Phys. Rev. D **108**, L061302 (2023).

[29] Javier F. Acevedo, Amit Bhoonah, and Joseph Bramante, Diffuse x-ray and gamma-ray limits on boson stars that interact with nuclei, J. Cosmol. Astropart. Phys. 12 (2022) 031.

[30] Nicolas Sanchis-Gual, Juan Calderón Bustillo, Carlos Herdeiro, Eugen Radu, José A. Font, Samson H. W. Leong, and Alejandro Torres-Forné, Impact of the wave-like nature of Proca stars on their gravitational-wave emission, Phys. Rev. D **106**, 124011 (2022).

[31] Jorge F. M. Delgado, Carlos A. R. Herdeiro, and Eugen Radu, Kerr black holes with synchronized axionic hair, Phys. Rev. D **103**, 104029 (2021).

[32] Nicolas Sanchis-Gual, Carlos Herdeiro, and Eugen Radu, Self-interactions can stabilize excited boson stars, Classical Quantum Gravity **39**, 064001 (2022).

[33] Marco Brito, Carlos Herdeiro, Eugen Radu, Nicolas Sanchis-Gual, and Miguel Zilhão, Stability and physical properties of spherical excited scalar boson stars, Phys. Rev. D **107**, 084022 (2023).

[34] Carlos Herdeiro, Eugen Radu, and Etevaldo dos Santos Costa Filho, Proca-Higgs balls and stars in a UV completion for Proca self-interactions, J. Cosmol. Astropart. Phys. 05 (2023) 022.

[35] Ivo Sengo, Pedro V. P. Cunha, Carlos A. R. Herdeiro, and Eugen Radu, Kerr black holes with synchronised Proca hair: Lensing, shadows and EHT constraints, J. Cosmol. Astropart. Phys. 01 (2023) 047.

[36] Juan Calderon Bustillo, Nicolas Sanchis-Gual, Samson H. W. Leong, Koustav Chandra, Alejandro Torres-Forne, Jose A. Font, Carlos Herdeiro, Eugen Radu, Isaac C. F. Wong, and Tjonnie G. F. Li, Searching for vector boson-star

mergers within LIGO-Virgo intermediate-mass black-hole merger candidates, Phys. Rev. D **108**, 123020 (2023).
[37] Vitor Cardoso, Taishi Ikeda, Zhen Zhong, and Miguel Zilhão, Piercing of a boson star by a black hole, Phys. Rev. D **106**, 044030 (2022).
[38] Rodrigo Vicente and Vitor Cardoso, Dynamical friction of black holes in ultralight dark matter, Phys. Rev. D **105**, 083008 (2022).
[39] Lorenzo Annulli, Vitor Cardoso, and Rodrigo Vicente, Response of ultralight dark matter to supermassive black holes and binaries, Phys. Rev. D **102**, 063022 (2020).
[40] Taishi Ikeda, Vitor Cardoso, and Miguel Zilhão, Instabilities of scalar fields around oscillating stars, Phys. Rev. Lett. **127**, 191101 (2021).
[41] Chen Yuan, Richard Brito, and Vitor Cardoso, Probing ultralight dark matter with future ground-based gravitational-wave detectors, Phys. Rev. D **104**, 044011 (2021).
[42] Taishi Ikeda, Richard Brito, and Vitor Cardoso, Blasts of light from axions, Phys. Rev. Lett. **122**, 081101 (2019).
[43] Vitor Cardoso, Óscar J. C. Dias, Gavin S. Hartnett, Matthew Middleton, Paolo Pani, and Jorge E. Santos, Constraining the mass of dark photons and axion-like particles through black-hole superradiance, J. Cosmol. Astropart. Phys. 03 (2018) 043.
[44] Richard Brito and Paolo Pani, Black-hole superradiance: Searching for ultralight bosons with gravitational waves, 10.1007/978-981-15-4702-7_37-1 (2021).
[45] Basabendu Barman, Debasish Borah, Arnab Dasgupta, and Anish Ghoshal, Probing high scale Dirac leptogenesis via gravitational waves from domain walls, Phys. Rev. D **106**, 015007 (2022).
[46] Jeff A. Dror, Takashi Hiramatsu, Kazunori Kohri, Hitoshi Murayama, and Graham White, Testing the seesaw mechanism and leptogenesis with gravitational waves, Phys. Rev. Lett. **124**, 041804 (2020).
[47] Simone Blasi, Vedran Brdar, and Kai Schmitz, Fingerprint of low-scale leptogenesis in the primordial gravitational-wave spectrum, Phys. Rev. Res. **2**, 043321 (2020).
[48] Bartosz Fornal and Barmak Shams Es Haghi, Baryon and lepton number violation from gravitational waves, Phys. Rev. D **102**, 115037 (2020).
[49] Rome Samanta and Satyabrata Datta, Gravitational wave complementarity and impact of NANOGrav data on gravitational leptogenesis, J. High Energy Phys. 05 (2021) 211.
[50] Felipe F. Freitas, Carlos A. R. Herdeiro, António P. Morais, António Onofre, Roman Pasechnik, Eugen Radu, Nicolas Sanchis-Gual, and Rui Santos, Ultralight bosons for strong gravity applications from simple standard model extensions, J. Cosmol. Astropart. Phys. 12 (2021) 047.
[51] Edward Seidel and Wai-Mo Suen, Formation of solitonic stars through gravitational cooling, Phys. Rev. Lett. **72**, 2516 (1994).
[52] Nitsan Bar, Diego Blas, Kfir Blum, and Sergey Sibiryakov, Galactic rotation curves versus ultralight dark matter: Implications of the soliton-host halo relation, Phys. Rev. D **98**, 083027 (2018).
[53] Nitsan Bar, Kfir Blum, Joshua Eby, and Ryosuke Sato, Ultralight dark matter in disk galaxies, Phys. Rev. D **99**, 103020 (2019).
[54] Don N. Page, Classical and quantum decay of oscillatons: Oscillating self-gravitating real scalar field solitons, Phys. Rev. D **70**, 023002 (2004).
[55] Richard Brito, Shrobana Ghosh, Enrico Barausse, Emanuele Berti, Vitor Cardoso, Irina Dvorkin, Antoine Klein, and Paolo Pani, Stochastic and resolvable gravitational waves from ultralight bosons, Phys. Rev. Lett. **119**, 131101 (2017).
[56] Richard Brito, Shrobana Ghosh, Enrico Barausse, Emanuele Berti, Vitor Cardoso, Irina Dvorkin, Antoine Klein, and Paolo Pani, Gravitational wave searches for ultralight bosons with LIGO and LISA, Phys. Rev. D **96**, 064050 (2017).
[57] Chen Yuan, Yang Jiang, and Qing-Guo Huang, Constraints on an ultralight scalar boson from Advanced LIGO and Advanced Virgo's first three observing runs using the stochastic gravitational-wave background, Phys. Rev. D **106**, 023020 (2022).
[58] Ken K. Y. Ng, Salvatore Vitale, Otto A. Hannuksela, and Tjonnie G. F. Li, Constraints on ultralight scalar bosons within black hole spin measurements from the LIGO-Virgo GWTC-2, Phys. Rev. Lett. **126**, 151102 (2021).
[59] Yoshihiko Abe, Takashi Toma, and Koichi Yoshioka, Nonthermal production of PNGB dark matter and inflation, J. High Energy Phys. 03 (2021) 130.
[60] Christian Gross, Oleg Lebedev, and Takashi Toma, Cancellation mechanism for dark-matter–nucleon interaction, Phys. Rev. Lett. **119**, 191801 (2017).
[61] Eduard Masso, Francesc Rota, and Gabriel Zsembinszki, Planck-scale effects on global symmetries: Cosmology of pseudo-Goldstone bosons, Phys. Rev. D **70**, 115009 (2004).
[62] Davide Cadamuro and Javier Redondo, Cosmological bounds on pseudo Nambu-Goldstone bosons, J. Cosmol. Astropart. Phys. 02 (2012) 032.
[63] JiJi Fan, Ultralight repulsive dark matter and BEC, Phys. Dark Universe **14**, 84 (2016).
[64] Georges Aad *et al.* (ATLAS Collaboration), Combination of searches for Higgs boson pairs in pp collisions at $\sqrt{s} =$ 13 TeV with the ATLAS detector, Phys. Lett. B **800**, 135103 (2020).
[65] T. Robens, Extended scalar sectors at current and future colliders, in *Proceedings of the 55th Rencontres de Moriond on QCD and High Energy Interactions* (2021), arXiv:2105.07719.
[66] Keir K. Rogers and Hiranya V. Peiris, Strong bound on canonical ultralight axion dark matter from the Lyman-Alpha forest, Phys. Rev. Lett. **126**, 071302 (2021).
[67] Alex Laguë, Bodo Schwabe, Renée Hložek, David J. E. Marsh, and Keir K. Rogers, Cosmological simulations of mixed ultralight dark matter, Phys. Rev. D **109**, 043507 (2024).
[68] Renée Hlozek, Daniel Grin, David J. E. Marsh, and Pedro G. Ferreira, A search for ultralight axions using precision cosmological data, Phys. Rev. D **91**, 103512 (2015).
[69] Alberto Diez-Tejedor and David J. E. Marsh, Cosmological production of ultralight dark matter axions, arXiv:1702.02116.
[70] L. F. Abbott and P. Sikivie, A cosmological bound on the invisible axion, Phys. Lett. **120B**, 133 (1983).

[71] John Preskill, Mark B. Wise, and Frank Wilczek, Cosmology of the invisible axion, Phys. Lett. **120B**, 127 (1983).

[72] Michael Dine and Willy Fischler, The not so harmless axion, Phys. Lett. **120B**, 137 (1983).

[73] Fatemeh Elahi and Sara Khatibi, Light non-Abelian vector dark matter produced through vector misalignment, Phys. Lett. B **843**, 138050 (2023).

[74] Sang Hui Im and Kwang Sik Jeong, Freeze-in axion-like dark matter, Phys. Lett. B **799**, 135044 (2019).

[75] Pierluca Carenza, Massimiliano Lattanzi, Alessandro Mirizzi, and Francesco Forastieri, Thermal axions with multi-eV masses are possible in low-reheating scenarios, J. Cosmol. Astropart. Phys. 07 (2021) 031.

[76] Edward Kolb, *The Early Universe* (CRC Press, Boca Raton, 2018).

[77] Masahiro Kawasaki, Ken'ichi Saikawa, and Toyokazu Sekiguchi, Axion dark matter from topological defects, Phys. Rev. D **91**, 065014 (2015).

[78] Takashi Hiramatsu, Masahiro Kawasaki, Ken'ichi Saikawa, and Toyokazu Sekiguchi, Axion cosmology with long-lived domain walls, J. Cosmol. Astropart. Phys. 01 (2013) 001.

[79] Maíra Dutra, Vinícius Oliveira, C. A. de S. Pires, and Farinaldo S. Queiroz, A model for mixed warm and hot right-handed neutrino dark matter, J. High Energy Phys. 10 (2021) 005.

[80] Amol V. Patwardhan, George M. Fuller, Chad T. Kishimoto, and Alexander Kusenko, Diluted equilibrium sterile neutrino dark matter, Phys. Rev. D **92**, 103509 (2015).

[81] Joel R. Primack and Michael A. K. Gross, Hot dark matter in cosmology, arXiv:astro-ph/0007165.

[82] Lawrence J. Hall, Karsten Jedamzik, John March-Russell, and Stephen M. West, Freeze-in production of FIMP dark matter, J. High Energy Phys. 03 (2010) 080.

[83] Lam Hui, Wave dark matter, Annu. Rev. Astron. Astrophys. **59**, 247 (2021).

[84] G. W. Gibbons and S. W. Hawking, Cosmological event horizons, thermodynamics, and particle creation, Phys. Rev. D **15**, 2738 (1977).

[85] P. A. R. Ade *et al.* (BICEP2 and Planck Collaborations), Joint analysis of BICEP2/*KeckArray* and *Planck* data, Phys. Rev. Lett. **114**, 101301 (2015).

[86] Shamit Kachru, Renata Kallosh, Andrei D. Linde, and Sandip P. Trivedi, De Sitter vacua in string theory, Phys. Rev. D **68**, 046005 (2003).

[87] Jerome Martin, Christophe Ringeval, and Vincent Vennin, Encyclopædia inflationaris, Phys. Dark Universe **5–6**, 75 (2014).

[88] Pierre Sikivie, Axion cosmology, Lect. Notes Phys. **741**, 19 (2008).

[89] A. Vilenkin and E. P. S. Shellard, *Cosmic Strings and Other Topological Defects* (Cambridge University Press, Cambridge, England, 2000).

[90] Ya. B. Zeldovich, I. Yu. Kobzarev, and L. B. Okun, Cosmological consequences of the spontaneous breakdown of discrete symmetry, Zh. Eksp. Teor. Fiz. **67**, 3 (1974).

[91] Paola Arias, Davide Cadamuro, Mark Goodsell, Joerg Jaeckel, Javier Redondo, and Andreas Ringwald, WISPy cold dark matter, J. Cosmol. Astropart. Phys. 06 (2012) 013.

[92] Luca Visinelli and Paolo Gondolo, Dark matter axions revisited, Phys. Rev. D **80**, 035024 (2009).

[93] Michael S. Turner, Cosmic and local mass density of invisible axions, Phys. Rev. D **33**, 889 (1986).

[94] Kyu Jung Bae, Ji-Haeng Huh, and Jihn E. Kim, Update of axion CDM energy, J. Cosmol. Astropart. Phys. 09 (2008) 005.

[95] P. A. Zyla *et al.* (Particle Data Group), Review of particle physics, Prog. Theor. Exp. Phys. **2020**, 083C01 (2020).

[96] Alexander Vilenkin, Cosmic strings and domain walls, Phys. Rep. **121**, 263 (1985).

[97] Mario Reig, José W. F. Valle, and Masaki Yamada, Light Majoron cold dark matter from topological defects and the formation of boson stars, J. Cosmol. Astropart. Phys. 09 (2019) 029.

[98] Richard Lynn Davis, Cosmic axions from cosmic strings, Phys. Lett. B **180**, 225 (1986).

[99] Richard Lynn Davis, Goldstone bosons in string models of galaxy formation, Phys. Rev. D **32**, 3172 (1985).

[100] Takashi Hiramatsu, Masahiro Kawasaki, Toyokazu Sekiguchi, Masahide Yamaguchi, and Jun'ichi Yokoyama, Improved estimation of radiated axions from cosmological axionic strings, Phys. Rev. D **83**, 123531 (2011).

[101] Takashi Hiramatsu, Masahiro Kawasaki, Ken'ichi Saikawa, and Toyokazu Sekiguchi, Production of dark matter axions from collapse of string-wall systems, Phys. Rev. D **85**, 105020 (2012); Phys. Rev. D **86**, 089902(E) (2012).

[102] P. Sikivie, Axions, domain walls, and the early universe, Phys. Rev. Lett. **48**, 1156 (1982).

[103] Takashi Hiramatsu, Masahiro Kawasaki, and Ken'ichi Saikawa, Evolution of string-wall networks and axionic domain wall problem, J. Cosmol. Astropart. Phys. 08 (2011) 030.

[104] Graciela B. Gelmini, Marcelo Gleiser, and Edward W. Kolb, Cosmology of biased discrete symmetry breaking, Phys. Rev. D **39**, 1558 (1989).

[105] Andrea Caputo and Mario Reig, Cosmic implications of a low-scale solution to the axion domain wall problem, Phys. Rev. D **100**, 063530 (2019).

[106] Marco Gorghetto and Edward Hardy, Post-inflationary axions: A minimal target for axion haloscopes, J. High Energy Phys. 05 (2023) 030.

[107] Sebastian E. Larsson, Subir Sarkar, and Peter L. White, Evading the cosmological domain wall problem, Phys. Rev. D **55**, 5129 (1997).

[108] Takashi Hiramatsu, Masahiro Kawasaki, and Ken'ichi Saikawa, On the estimation of gravitational wave spectrum from cosmic domain walls, J. Cosmol. Astropart. Phys. 02 (2014) 031.

[109] Ken'ichi Saikawa, A review of gravitational waves from cosmic domain walls, Universe **3**, 40 (2017).

[110] Yang Bai, Ting-Kuo Chen, and Mrunal Korwar, QCD-collapsed domain walls: QCD phase transition and gravitational wave spectroscopy, J. High Energy Phys. 12 (2023) 194.

[111] Konstantin A. Beyer and Subir Sarkar, Ruling out light axions: The writing is on the wall, SciPost Phys. **15**, 003 (2023).

[112] Graciela B. Gelmini, Anna Simpson, and Edoardo Vitagliano, Gravitational waves from axionlike particle

cosmic string-wall networks, Phys. Rev. D **104**, 061301 (2021).
[113] Graciela B. Gelmini, Anna Simpson, and Edoardo Vitagliano, Catastrogenesis: DM, GWs, and PBHs from ALP string-wall networks, J. Cosmol. Astropart. Phys. 02 (2023) 031.
[114] Alejandro Vaquero, Javier Redondo, and Julia Stadler, Early seeds of axion miniclusters, J. Cosmol. Astropart. Phys. 04 (2019) 012.
[115] Kenji Kadota, Masahiro Kawasaki, and Ken'ichi Saikawa, Gravitational waves from domain walls in the next-to-minimal supersymmetric standard model, J. Cosmol. Astropart. Phys. 10 (2015) 041.
[116] Juan Garcia-Bellido, Hitoshi Murayama, and Graham White, Exploring the early universe with GAIA and THEIA, J. Cosmol. Astropart. Phys. 12 (2021) 023.
[117] A. Weltman *et al.*, Fundamental physics with the square kilometre array, Publ. Astron. Soc. Aust. **37**, e002 (2020).
[118] Pau Amaro-Seoane, Heather Audley, Stanislav Babak, John Baker, Enrico Barausse, Peter Bender, Emanuele Berti, Pierre Binetruy, Michael Born, Daniele Bortoluzzi *et al.*, Laser interferometer space antenna, arXiv:1702.00786.
[119] Alberto Sesana *et al.*, Unveiling the gravitational universe at μ-Hz frequencies, Exp. Astron. **51**, 1333 (2021).
[120] Kent Yagi and Naoki Seto, Detector configuration of DECIGO/BBO and identification of cosmological neutron-star binaries, Phys. Rev. D **83**, 044011 (2011); Phys. Rev. D **95**, 109901(E) (2017).
[121] J. Aasi *et al.* (LIGO Scientific Collaboration), Advanced LIGO, Classical Quantum Gravity **32**, 074001 (2015).
[122] M. Punturo *et al.*, The Einstein Telescope: A third-generation gravitational wave observatory, Classical Quantum Gravity **27**, 194002 (2010).